2014 23rd International Lightning Detection Conference
18 - 19 March • Tucson, Arizona, USA
5th International Lightning Meteorology Conference
20 - 21 • Tucson, Arizona, USA

An Intrinsic Fiber-Optic Sensor for Structure Lightning Current Measurement

Truong X. Nguyen, Jay J. Ely and
George N. Szatkowski
NASA Langley Research Center
Hampton, VA 23681 U.S.A.
truong.x.nguyen@nasa.gov

Carlos T. Mata and Angel G. Mata
ESC - Kennedy Space Center, FL 32899 U.S.A

Gary P. Snyder
NASA - Kennedy Space Center, FL 32899 U.S.A.

***Abstract*— An intrinsic optical-fiber sensor based on Faraday Effect is developed that is highly suitable for measuring lightning current on aircraft, towers and complex structures. Originally developed specifically for aircraft installations, it is light-weight, non-conducting, structure conforming, and is immune to electromagnetic interference, hysteresis and saturation. It can measure total current down to DC. When used on lightning towers, the sensor can help validate other sensors and lightning detection network measurements.**

Faraday Effect causes light polarization to rotate when the fiber is exposed to a magnetic field in the direction of light propagation. Thus, the magnetic field strength can be determined from the light polarization change. By forming closed fiber loops and applying Ampere's law, measuring the total light rotation yields the total current enclosed. A broadband, dual-detector, reflective polarimetric scheme allows measurement of both DC component and AC waveforms with a 60 dB dynamic range.

Two systems were built that are similar in design but with slightly different sensitivities. The 1310nm laser system can measure 300 A - 300 kA, and has a 15m long sensing fiber. It was used in laboratory testing, including measuring current on an aluminum structure simulating an aircraft fuselage or a lightning tower. High current capabilities were demonstrated up to 200 kA at a lightning test facility. The 1550nm laser system can measure 400 A - 400 kA and has a 25m fiber length. Used in field measurements, excellent results were achieved in the summer of 2012 measuring rocket-triggered lightning at the International Center for Lightning Research and Testing (ICLRT), Camp Blanding, Florida. In both systems increased sensitivity can be achieved with multiple fiber loops.

The fiber optic sensor provides many unique capabilities not currently possible with traditional sensors. It represents an important new tool for lightning current measurement where low weight, complex shapes, large structure dimension, large current, and low frequency capabilities are important considerations.

Keywords—lightning; Faraday Effect; current sensor; fiber-optic; aircraft; direct measurement;

I. INTRODUCTION

Accurate characterization of lightning return stroke current is important in protection against direct and indirect effects. As described in literature, methods to characterize lightning currents typically include indirect remote measurements using various field sensors, or direct measurements using rocket-triggered setups and instrumented towers. Direct measurement also includes flight campaigns characterizing aircraft in-flight lightning environment [1,2]. Data from direct measurements are much more limited but are more accurate and often used in validation of indirect measurement setups.

Direct measurement typically utilizes traditional sensors such as resistive current shunt, Rogowski coil, current transformer, or time-derivative sensor (i.e. I-Dot), each with its own advantages. However, depending on applications these sensors may have installation restrictions, such as size and weight, or have performance limitations such as amplitude range, frequency, bandwidth, saturation or hysteresis. These limitations can be difficult to overcome especially for aircraft external installations where there are considerations for aerodynamic performance, safety, weight, and installation cost.

An on-going effort to characterize aircraft lightning environment led to the development of a fiber-optic current sensor tailored for direct lightning measurement. It has most of the advantages of traditional sensors and with few disadvantages. Desirable characteristics are many, including being light weight, flexible, and conforming to structure geometries. It is self-integrating and can measure total current (not the time derivatives) including the DC component. It does not suffer from self-resonance, saturation or hysteresis as with Rogowski coil or current transformer. It is not susceptible to arcing/sparking from high voltage and current. Being non-conductive, the sensor can be safely routed directly into an aircraft fuselage or a control room.

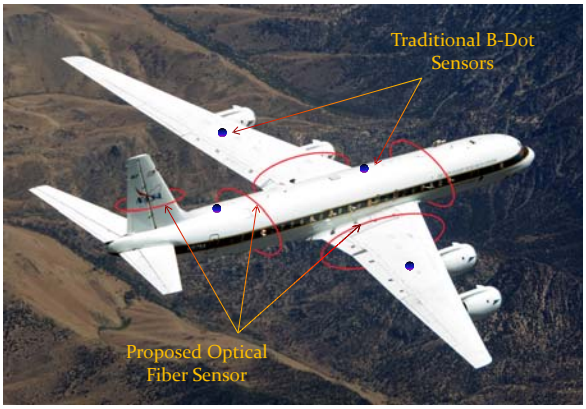

NASA Illustration 2012

Fig. 1. Illustration of fiber-optic current sensors on aircraft.

Sensor installation is simple and non-intrusive, simply by wrapping the thin fiber one or more times around the structure to be measured. Versatility is excellent, as the same sensing fiber can be used on small or large structures. The results would be accurate in both cases given sufficient bandwidth and length. Measurement sensitivity can be increased by using multiple fiber-turns around the conductor.

Aircraft installation would benefit the most from this new sensor due to strict size, weight, aerodynamic performance and safety requirements. Fig. 1 illustrates possible fiber installations measuring current on structures such as fuselage, wings, or tail sections. To date the sensor has not yet been flown on an aircraft due to typical high costs for any flight experiment, and that most aircraft would avoid flying into thunderstorms intentionally. Regardless, this sensor represent a significant leap in capabilities relative to traditional sensors used in past flight experiments. The sensor's many advantages could benefit other direct lightning measurements such as on small buildings, windmills, or lightning towers as illustrated in Fig. 2.

The sensor is based on Faraday (Rotation) Effect, which causes light's polarization plane in a medium to rotate when the medium is exposed to a magnetic field in the direction of light propagation. Using optical fiber as the propagation medium and by forming close fiber loops, measuring the total light rotation would result in the total current enclosed. It is noted that the sensing element is an optical fiber, thus termed "intrinsic" sensor. In contrast, in "extrinsic" sensor optical fiber is only used for relaying signal from a remote sensor.

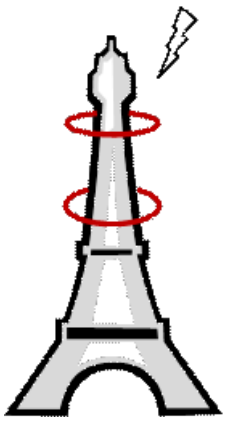

Fig. 2. Fiber-optic current sensors loops on a lightning tower.

The sensor is not without limitations. Fiber choice is limited. Most commonly available fibers are based on silica, and the Faraday Effect in silica is weak. However, this makes the sensor highly suitable for large currents such as in lightning. There are slight temperature and bend/vibration sensitivities, though there are approaches to compensate, in real-time or through post processing, that could lead to very precise measurements. Glass fiber is also fragile and needs suitable protection.

This paper describes two sensor systems that are similar in design and characteristics, only with slightly different measurement ranges. Their lasers operate at 1310nm and 1550nm wavelengths where optical components are relatively commonly available. In this paper the 1310nm system was used in laboratory demonstrations while the 1550nm system for field measurement of triggered lightning. Their design is described in the next section. In addition, measurement results are reported for:

- Equivalent current up to 300 kA, using multiple fiber loops or a multi-turn current coil.
- Current on a 1.2 m diameter round structure emulating a miniature lightning tower or an aircraft fuselage.
- Large current having 100 kA and 200 kA peaks, performed at a commercial lightning test facility.
- Triggered-lightning currents at the International Center for Lightning Research and Testing (ICLRT), at Camp Blanding, Florida.

These tests and results illustrate the ability to measure large direct lightning current on structures. The fiber-optic current sensor is simply referred to as Faraday sensor in the remainder of the paper.

II. FIBER-OPTIC CURRENT SENSOR

A. *Basic Sensor Operation*

As stated, Faraday Effect causes light polarization in an optical medium to rotate when the medium is exposed to a magnetic field in the direction of light propagation. The effect in an optical fiber is illustrated in Fig. 3. The amount of rotation depends on the material and the strength of the magnetic field component. The polarization plane rotation, in radians, is [3-10]:

$$\phi = V \int \boldsymbol{B} \cdot d\boldsymbol{l} = \mu_0 V \int \boldsymbol{H} \cdot d\boldsymbol{l}\,, \tag{1}$$

where μ_0 is the free-space permeability; V is the Verdet constant in radians/(meter·Tesla); $\mu_0 V$ is the combined permeability Verdet constant (radians/ampere); **B** is magnetic flux density in Tesla (T); length *l* (in meters) is the light and

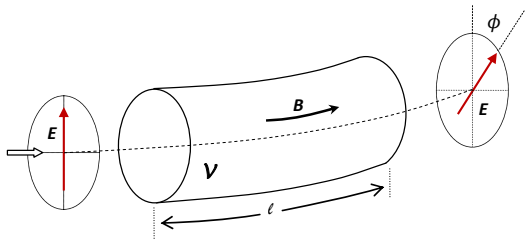

Fig. 3. Faraday Effect in optical fiber.

magnetic field interaction path length; and **H** is the magnetic field (amperes/meter). For a fiber forming N closed loops around a conductor carrying current I (ampere), applying Ampere's law yields

$$\phi = \mu_0 V \oint \boldsymbol{H} \cdot d\boldsymbol{l}\,, \quad = \mu_0 VNI \tag{2}$$

Thus, the rotation angle is directly proportional to the current I and the number of loops N. The sensor is self-integrating, and no additional integration is needed. Measuring the rotation angle directly results in current, knowing the number loops used.

B. Polarimetric Detection Scheme

This section describes the scheme used to measure the polarization change induced by current. The scheme is illustrated in Fig. 4 [4]. A linearly polarized light from a super-luminescence diode (SLD) laser is generated at locations labeled 1, 2. Half of the power is transmitted through the non-polarizing beam splitter (NBS) at 3 to the sensing fiber at 4. The sensing fiber forms closed loops around the current carrying conductor at 5. A Faraday mirror at 6 rotates the reflected light polarization by 90º relative to the incident light. This helps cancel fiber bend/stress induced effects and makes the sensor less sensitive to bending. The reflected light traces back through the fiber to 3, at which half of the power is reflected through the half-wave plate (HWP) at 7 toward the polarizing beam splitter (PBS) at 8. Exiting the PBS, light power in the two orthogonal polarizations are measured by two photo-detectors D1 and D2 at 9. The HWP helps rotate and align the initial polarization incident on the PBS. Ideally, at zero current the incident polarization should be at 45º relative to the PBS's two orthogonal principle polarization axes, so that beam power is divided equally between the two optical detectors at 9. The difference in optical powers at 9 is measured with a balanced detector.

This setup is referred to as a reflective scheme, since a mirror is incorporated. Using this scheme in combination with a Faraday mirror, as light travels through the fiber twice, the non-reciprocal Faraday rotation is doubled while external stress-induced effects are subtracted [5].

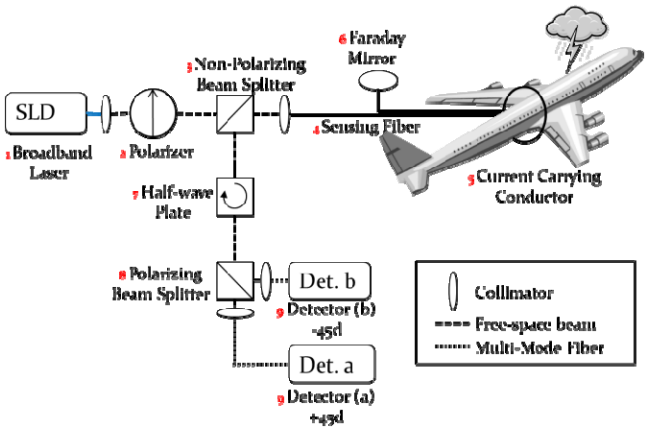

Fig. 4. Reflective polarimetric scheme with dual detectors.

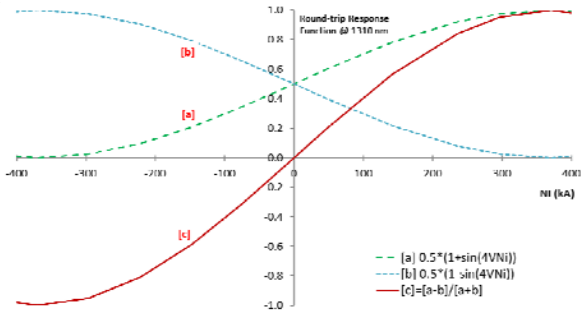

Fig. 5. Ideal sensor responses at 1310 nm.

The responses at the two detectors should ideally be (a),(b)=0.5*[1±*sin*($4\mu_0$VNI)] for a reflective scheme. Mathematic operation difference-over-sum, (c)=(a-b)/(a+b), yields

$$(c) \;=\; sin\,(4\mu_0 VNI), \text{ or} \tag{3}$$

$$NI \;=\; sin^{-1}(c)/\,(4\mu_0 V), \tag{4}$$

where *equivalent current* NI (in unit Ampere-turn) is defined as number of loops N times the current I, and $\mu_0 V$ = 1.01 μrad/A at 1310nm and 0.718 μrad/A at 1550nm [3].

It is important that light's linear state-of-polarization is maintained in the fiber during light transit. This is achieved with proper fiber design. The systems in this paper use two different commercial spun polarization-maintaining (PM) fibers [6], which are the result of twisting PM fibers during manufacturing. Fiber twisting helps hold the state-of-polarization that otherwise would be destroyed in a typical fiber. The twist rate is about 5 mm per turn.

Fig. 5 illustrates the ideal responses at 1310nm, with the response curves (a) and (b) being voltage outputs from the two optical detectors. The difference-over-sum operation (c)=(a-b)/(a+b) would yield a response that is more sensitive (higher slope) than either response curve, with zero crossing at zero current, and has larger dynamic range due to common-mode noise subtraction. Current I or equivalent current NI is then computed from (c) using eq. (4).

The typical operating range is where the curve (c) increases monotonically in Fig. 5, or about -350 kA to +350 kA. In this range the response and current correspond one-to-one. In the systems described in this paper, non-ideal fiber medium and optical components distort the curves. The practical range is slightly reduced to about -300 kA to +300 kA as to be reported in the next section.

The 1550nm-based system is slightly less sensitive due to the lower Verdet constant at this wavelength, so it can measure slightly larger current. The practical range is approximately +/- 400 kA. The design, construction and characteristics otherwise are very similar to the previously described 1310 nm system.

Over-current would not damage the sensor - light polarization would simply rotate beyond the intended range. The concern is that the solution to the sin^{-1} function in (4)

would be ambiguous. However, there are simple solutions that permit measurement of very large current [7]. These techniques are not necessary here since most known direct lightning currents are below the 300 kA and 400 kA ranges of the two systems described.

C. *Sensor Calibration and Data Correction*

The 1310nm system was measured in laboratory and the results compared against reference sensors that include a Rogowski coil (with an electronic integrator) and a ferrite-based Pearson™ current transformer (CT). Fig. 6 compares the three sensors by plotting current from the Faraday sensors on the vertical axes against current from the reference sensors on the horizontal axes. Large equivalent currents were achieved with the help of multiple fiber turns or a wire coil. Details are described in the next section.

Ideally the Faraday sensor data would fall on the straight diagonal line labeled "ideal". This line represents (1:1) correspondence between the Faraday sensor and the two reference sensors. Instead, the data follow the red curve labeled "uncorrected". This non-ideal response is due to the reduced sensitivity in the fiber (relative to ideal) along with light depolarization due to non-ideal fiber medium and optical components. Additional details concerning light propagation in spun fiber can be found in [7]. It is also clear that the uncorrected sensor's response is non-linear unless restricted to low current. Thus, it is important that the sensor is calibrated over its operating range and a correction function developed.

The correct function is developed from a simple polynomial spline-fit curve (5^{th} to 9^{th}, odd order) that maps the Faraday sensor response to the "ideal" curve. Once complete and verified the same correction function can be applied to subsequent measurements to achieve the corrected results. Fig. 6 shows the "corrected" response curve aligns well with the "ideal" diagonal line. An alternative to curve-fitting is interpolation; however, neither approach is perfect as some small error may remain.

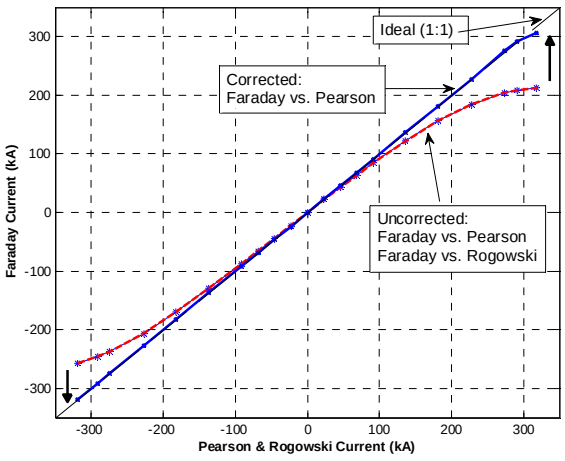

Fig. 6. The 1310nm system's response curve, corrected and un-corrected.

III. LABORATORY TEST RESULTS

It is difficult to achieve the full range test or calibration levels up to 300 kA (or 400 kA for the 1550nm system) in a laboratory setting. One acceptable approach is to produce the associated optical effects by using multiple fiber loops and/or a multi-turn conductor coil. Multiple fiber loops and wire turns amplify the Faraday rotation beyond that produced by a single fiber loop around a single conductor. The amplification factor is the product of the numbers of fiber loops and wire turns used. Fig. 7 illustrates a typical setup. Laboratory tests show using multiple fiber loops, a multi-turn coil, or combinations yield the same response curves.

For simplicity, N is redefined to be the product of the number of fiber loops and the number of wire turns. The product NI is simply referred to as equivalent current as previously stated in Eq. (4).

Fig. 8 illustrates excellent results comparison between the Faraday sensor and the reference sensors, with different number of fiber turns and wire loops. The equivalent currents NI are about 5 kA•turns and 300 kA•turns as shown. The same calibration correction function was used and good results were achieved in both cases. Since the reference Rogowski coil and Pearson current transformer (CT) only measure current on one wire-turn, their results are numerically scaled by the factor N for the comparison. This practice is commonly used in optical current sensing [3-10]. Similarly, NI up to 400 kA•turns was demonstrated with the 1550 nm wavelength system. Equally good results were achieved though not reported here.

In calibration setups to achieve high equivalent current, using a wire coil having a high number of turns can distort the injected waveform. This is illustrated by comparing Fig. 8(i) to 8(ii) - the pulse width in the former widens considerably. In contrast, using a high number of fiber loops does not affect the current waveform but would require a longer sensing fiber.

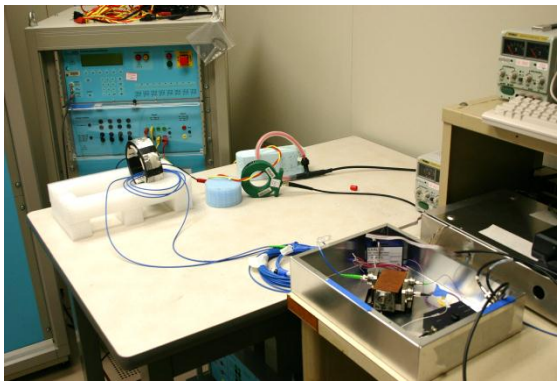

Fig. 7. Using multi-turn coil and multiple fiber loops to achieve high current effects.

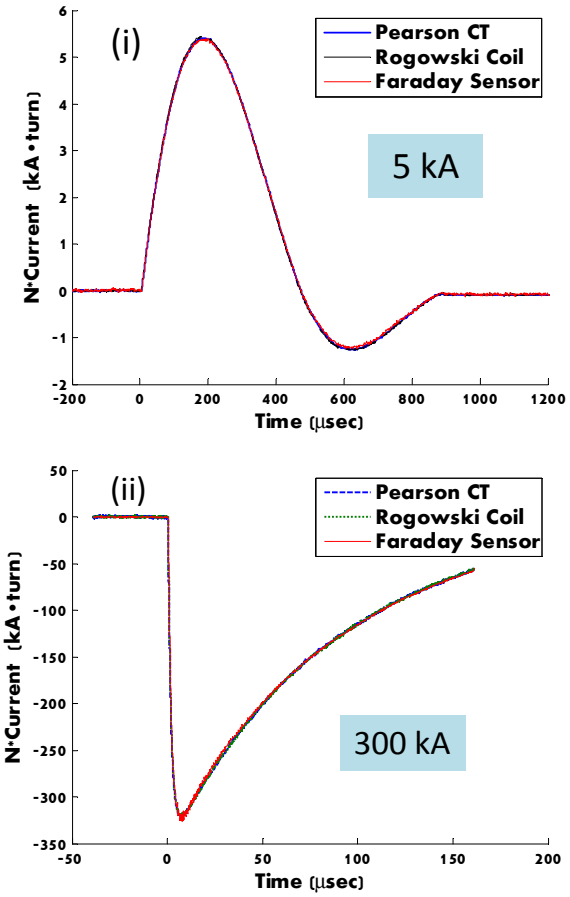

Fig. 8. Good equivalent current (N*I) result comparisons using (i) 49-turn coil and one fiber loop (N=49), and (ii) 3-turn coil and 28 fiber loops (N=3*28=84).

IV. DIRECT LARGE CURRENT MEASUREMENT

The 1310nm sensor system was evaluated for large current performance using only one fiber loop on one conductor (N=1). Using one fiber loop would be similar to installation external to an aircraft fuselage, a large structure, or a lightning tower. The tests were performed at a commercial lightning test facility, using standard aircraft lightning test waveforms that include components D, B and C [11]. Test current amplitudes were 20, 40, 100 and 200 kA. All were of double-exponential waveform, except for the 200 kA damped sinusoidal (limited by the test facility's abilities to generate unipolar waveforms). This test piggybacked on a separate effort to evaluate lightning effects on composite panels.

Fig. 9 illustrates the test setup. The Faraday sensor fiber formed one loop around the flat-plate return conductor as labeled. In an optimal setup both ends of the fiber loop would be co-routed away and exit the high magnetic field test zone. However, optimal setup was not achieved due to routing space restrictions. One end of the fiber was routed near the test zone into the shielded enclosure that housed the optical box and the data acquisition system. The other end was unable to form closed loop at the shielded enclosure and was simply formed a coil on the floor. Thus, a fiber section was exposed to high magnetic field whose effects would otherwise be canceled if a

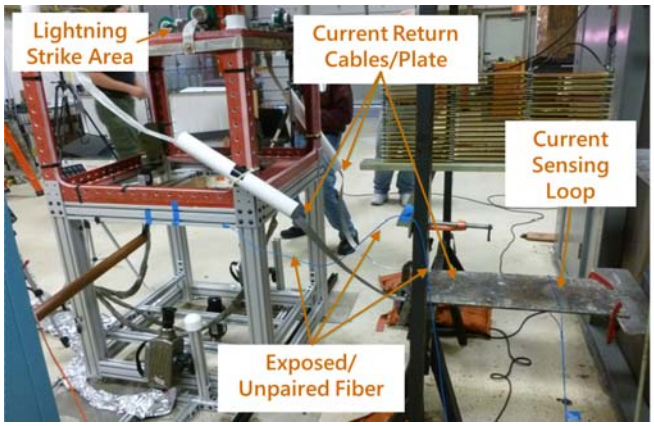

Fig. 9. Measuring large current with one fiber loop.

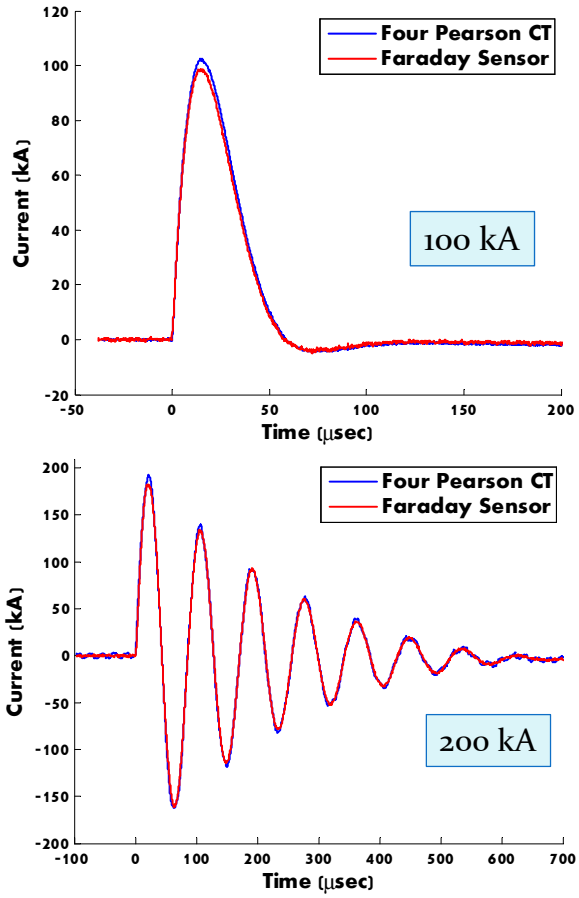

Fig. 10. Reasonable comparison achieved measuring large current (100 kA and 200 kA peaks) despite imperfect setup.

closed loop was achieved. Consequently, some measurement error was anticipated.

Fig. 10 shows results for 100 kA and 200 kA peak current against reference results. The reference results were the mathematical sums of four Pearson CTs outputs measuring current exiting the four sides of the composite panels.

The results are reasonably good considering the non-optimal fiber routing. The errors are about 3-10% depending

on the routing of the unpaired fiber section. These results demonstrate that the Faraday sensor is capable of directly measuring 200 kA current using just one loop, similar to expected structure installations.

V. LARGE STRUCTURE MEASUREMENT

Fig. 11 illustrates the setup measuring current on an aluminum cylinder that simulates a round lightning tower or an aircraft fuselage. Current lightning waveforms from 250 A to 4 kA were injected onto the cylinder at the bottom left location. The current amplitudes were limited by the laboratory equipment used. Return currents were extracted from the cylinder at bottom right.

The 15m fiber form a single fiber loop around the cylinder, with both ends co-routed to the optical box located 4m away on the table in the foreground. As can be seen in Fig. 11, the fiber closed the loop at the optical box without any unpaired fiber section, thus good isolation was achieved. A Pearson CT and a Rogowski coil provide reference comparison data. Fig. 12 shows good results for both the 250 A and 4 kA tests.

Noise is clearly visible in the 250 A measurement, illustrating the low level sensitivity limit. The dominant noise source is the SLD laser, which is a wideband noise source. Noise reduction techniques implemented include the balanced detector and a 1.9 MHz low-pass filter. In addition, moving-window data averaging is implemented in data post-processing with a small averaging window, i.e. 11 point window out of 10,000 points data length. A 60 dB range could be achieved with this setup.

VI. TRIGGERED LIGHTNING MEASUREMENT

Over the summer of 2012, the sensor system based on the 1550 nm wavelength was demonstrated measuring rocket-triggered lightning for a more realistic lightning environment. The test was performed at the ICLRT facility [12]. The measurement was similar to an earlier (2011) and successful effort utilizing a sensor system operating at 850nm laser wavelength and a twisted single-mode sensing fiber [13-15]. In the 2012 setup shown in Fig. 13, triggered lightning flashes would attach to the wire cage, and lightning current would travel to the ground via a resistive shunt (T&M Model R-7000-10) and a down-conductor. The sensing fiber formed four loops around the conductor. The remaining fiber segments at the two ends were co-routed radially away from the site. One end was connected to the optical box 12m away. The other end was connected to a Faraday mirror that was buried in the ground to minimize temperature variations.

Due to insufficient fiber length, the Faraday mirror was positioned only about 4m from the launch tubes rather than closing the loop near the optical box. Thus, about 8m (from the Faraday mirror to the optical box) section of the sensing fiber was "unpaired", potentially exposed to the effects of magnetic fields from the lightning flash and strong ground currents that would normally be canceled with a closed loop. However, by routing the fiber in the radial direction away from the lightning tower, magnetic field components in the direction of the fiber are expected to be minimized, reducing any undesirable effects. The fiber was protected from wild animals or being trampled on inside combinations of rain gutters and plastic braided sleeves (Figs. 13-14). Data were recorded using 14-bit digitizers at 100 MHz sampling rate. The sensors and digitizers were powered by batteries.

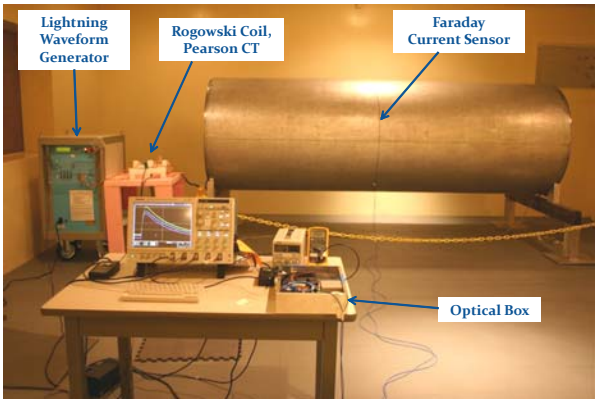

Fig. 11. Measurement on a large aluminum cylinder simulating an aircraft fuselage.

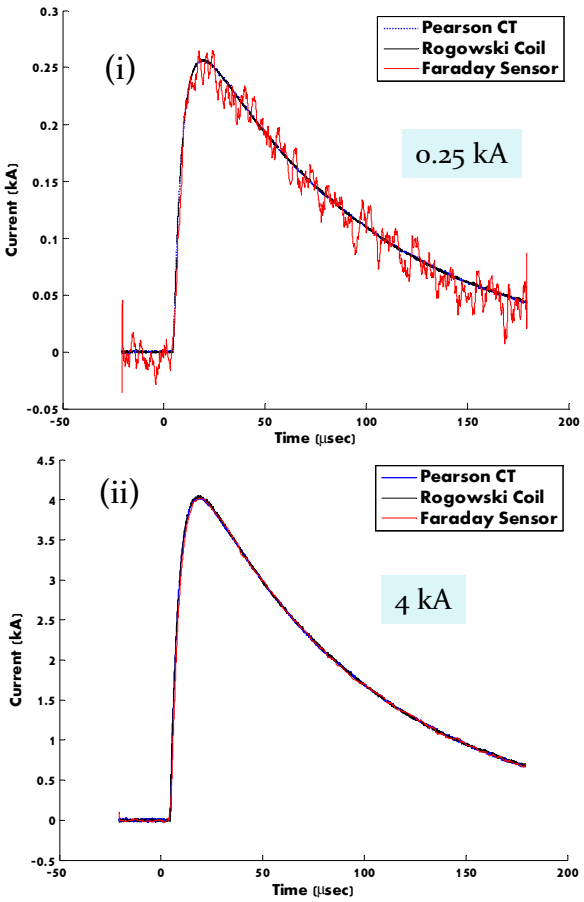

Fig. 12. Current measurement on a 1.2 m diameter cylinder.

Fig. 13. Four loops of fiber optic current sensor installed under the rocket launch tubes.

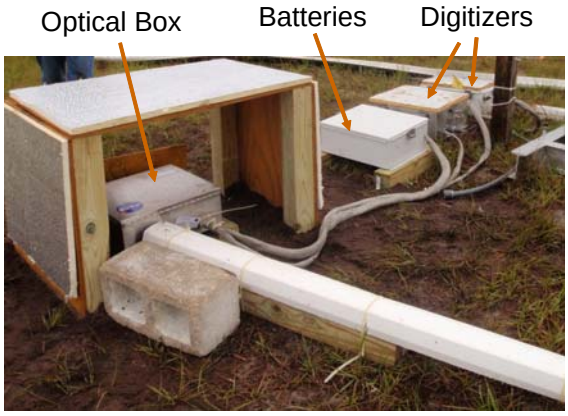

Fig. 14. Optical box and digitizers located 12m from the launch tower.

The 1550nm system is capable of measuring NI = 400 A to 400 kA range. To improve sensitivity, four fiber loops (N=4) were used. The current range (I) is effectively 100 A to 100 kA, which is reasonable for typical low peak lightning levels observed at the site.

Before any actual triggered lightning measurements, a series of verification tests were conducted comparing outputs from three different sensors: the Faraday sensor, the reference resistive shunt, and a current transformer. Several one kA positive and negative current waveforms were injected onto the wire cage that surrounded the rocket launch tubes while return currents were extracted from the base of the down-conductor. The results comparisons were excellent, verifying the accuracy of both the shunt resistor and the Faraday sensor. There was no ground current in this test setup as with actual lightning flashes.

Fig. 15 illustrates good result comparisons with the shunt resistor were achieved with actual triggered lightning. Electric current amplitude-versus-time waveforms are nearly identical between the two sensors. The long time scales chosen in the

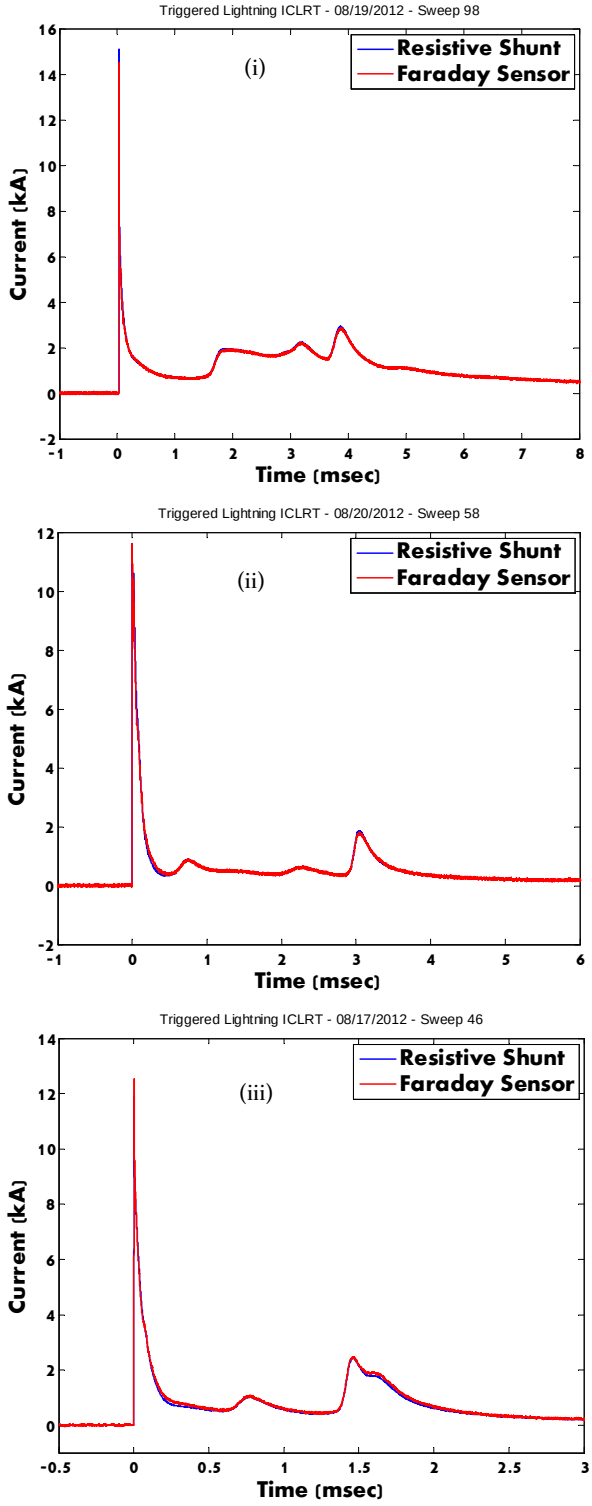

Fig. 15. Results for the 1550nm system show good comparisons with resistive shunt.

plots highlight the ability to measure long duration components such as continuing current. It is noted that the actual lightning currents I are reported in Fig. 15. The amplification effects from the multiple fiber loops are removed from the data.

As a side note, the system suffered from electromagnetic interference in early results due to strong ground currents,

affecting the peak measurements. In the later results as shown, interference became much less simply by slightly raising off the ground the data cables connecting the optical box to the data acquisition system. The cable spacing above ground was about 5 cm, supported underneath by a wood beam. Fig. 15(i) shows about 400A error in the peak currents relative to the resistive shunt. The remainder of the waveforms compare very well.

The interference problem could be further minimized in future setups that have strong ground current by having better cable shielding, by elevating the cables and/or setup higher above the ground, or by having the optical box and the digitizers in the same shielded enclosure. It is noted that ground current is not a problem for aircraft installations as equipment will be protected inside the fuselage.

VII. SENSOR BANDWIDTH

Bandwidth of a sensor system is limited by the lowest bandwidth of its components. For the fiber sensor component, it is limited by the light transit time in the interaction length of the fiber. This limitation is to ensure that the total transit time is much faster than the signal change rate for proper integration. The fiber interaction length includes the round-trip distance around the conductor and includes the distance to and from the Faraday sensor. The 3-dB sensor bandwidth (BW) is [3,4]: $BW \approx 0.44/t \approx 0.44c/nl$, where t is transit time, c is the speed of light in free space, n is the index of refraction in fiber material (n=1.5), and l is the interaction length (double of fiber length for reflective scheme).

Table I computes the maximum fiber length and structure dimensions for different bandwidths. Higher measurement bandwidth would require reduced structure size. Aircraft thin structures may include wings and tail surfaces, while round structures may include fuselage, etc. Since most of the lightning energy that can cause structure damage is contained in bandwidth far below one MHz, structures in excess of 14m diameter can be measured. This is sufficient even for the current largest passenger aircraft fuselage, at 7.8m diameter for the Airbus A380 model.

TABLE I. STRUCTURE DIMENSION VS. SENSOR BANDWIDTH

3-dB Bandwidth (MHz)	Max Fiber Length (m)	Max Thin Structure Dimension (m)	Max Round Structure Diameter (m)
1	44	22	14
2	22	11	7
4	11	5.5	3.5
10	4.4	2.2	1.4
20	2.2	1.1	0.7

VIII. CONCLUSION

The design, accuracy, advantages and versatility of fiber-optic current sensor are described and validated though multiple demonstrations. The measurements include large current up to 200 kA, current on large structure, and triggered lightning. Accurate equivalent current was achieved up to 300 kA and 400 kA for another for the two systems. Advantages such as structure conformity, total current measurement, non-conductivity, being light weight and many others make this sensor truly unique for direct lightning measurement.

IX. REFERENCES

[1] F. Pitts, B. Fisher, V. Mazur, and R. Perala, "Aircraft Jolts from Lightning Bolts," IEEE Spectrum, July 1988.

[2] P. Laroche, P. Blanchet, A. Delannoy, F. Issac, "Experimental Studies of Lightning Strikes to Aircraft," Onera Aerospace Lab Journal, Issue 5, December 2012 (AL05-06).

[3] J. M. Lopex-Higuera, Editor. Handbook of Optical Fibre Sensing Technology, 2002; Sections 27.2 - 27.4.

[4] G. Day, and A. Rose, "Faraday Effect Sensors: The State of the Art," Proc. SPIE, 1988, pp. 138–150.

[5] P. Drexler and P. Fiala,"Utilization of Faraday Mirror in Fiber Optic Current Sensors", Radioengineering, Vol. 17, Dec. 2008.

[6] R. Laming and D. Payne, "Electric Current Sensors Employing Spun Highly Birefringent Optical Fibers," Journal of Lightwave Technology, Dec. 1989.

[7] A. White, G. McHale, D. Goerz, "Advances in Optical Fiber-Based Faraday Rotation Diagnostics," 17th IEEE Int. Pulsed Power Conference, Wash. DC, July 2009 (LLNL-CONF-415198).

[8] A. Smith, "Polarization and Magneto-optic Properties of Single-Mode Optical Fiber," Applied Optic, Jan. 1978.

[9] R. Ulrich, and A. Simon, "Polarization Optics of Twisted Single-Mode Fibers," Applied Optics, Vol. 18, Issue 13, pp. 2241-2251 (1979).

[10] S. Rashleight, "Origins and Control of Polarization Effects in Single-Mode Fibers," Journal of Lightwave Technology, Vol. LT-1, No. 2, 1983.

[11] ARP-5412 "Aircraft Lightning Environment and Related Test Waveforms," Rev B, Jan 2012.

[12] V. Rakov, "A review of Triggered-Lightning Experiments," 30th International Conference on Lightning Protection, Cagliari, Italy, September 13-17, 2010.

[13] T. Nguyen, and G. Szatkowski, "Fiber Optic Sensor for Aircraft Lightning Current Measurement", ICOLSE, 2011.

[14] T. Nguyen, J. Ely, G. Szatkowski, C. Mata, A. Mata, G. Snyder, "Fiber-Optic Sensor for Aircraft Lightning Current Measurement," 2012 Int. Conf. on Lightning Protection (ICLP).

[15] T. Nguyen, J. Ely, G. Szatkowski, C. Mata, A. Mata, G. Snyder, "Fiber-Optic Current Sensor Validation with Triggered Lightning Measurements," 2013 Int. Conf. on Lightning and Static Electricity (ICOLSE).

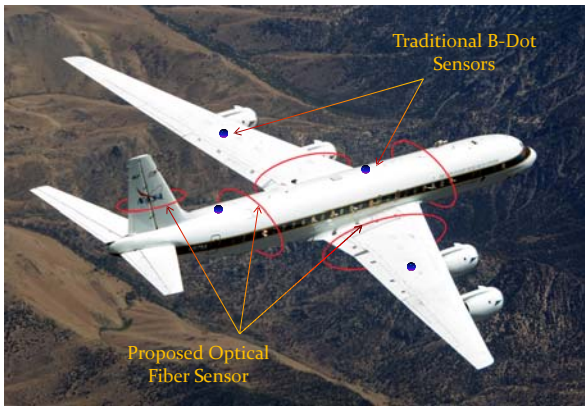

NASA Illustration 2012

Fig. 1. Illustration of fiber-optic current sensors on aircraft.

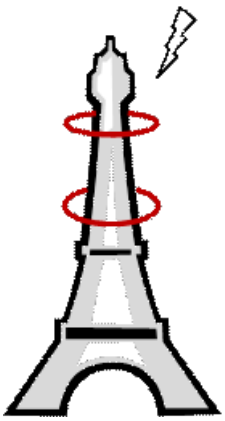

Fig. 2. Fiber-optic current sensors loops on a lightning tower.

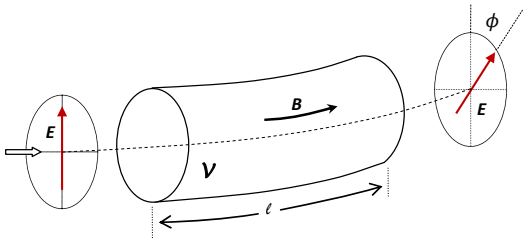

Fig. 3. Faraday Effect in optical fiber.

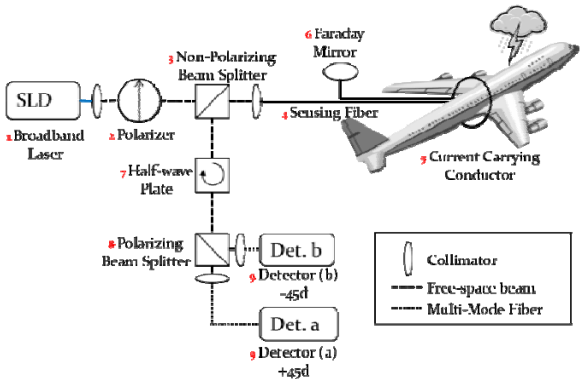

Fig. 4. Reflective polarimetric scheme with dual detectors.

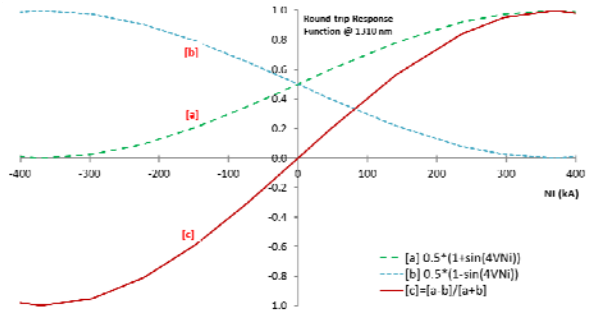

Fig. 5. Ideal sensor responses at 1310 nm.

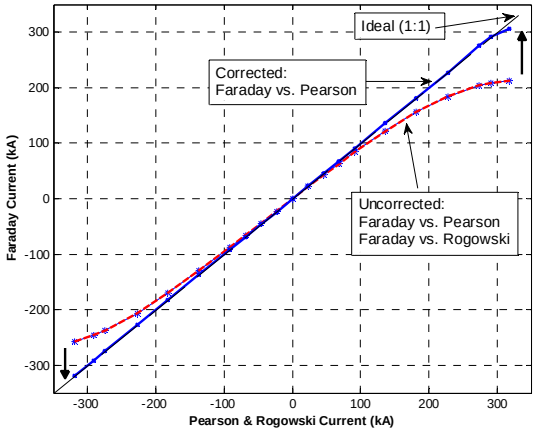

Fig. 6. The 1310nm system's response curve, corrected and uncorrected.

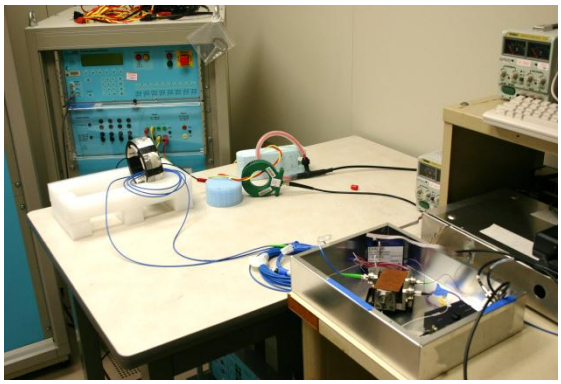

Fig. 7. Using multi-turn coil and multiple fiber loops to achieve high current effects.

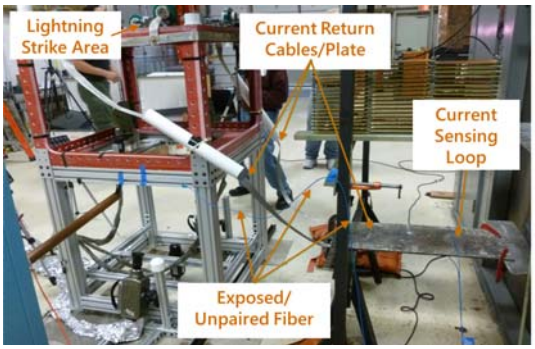

Fig. 9. Measuring large current with one fiber loop.

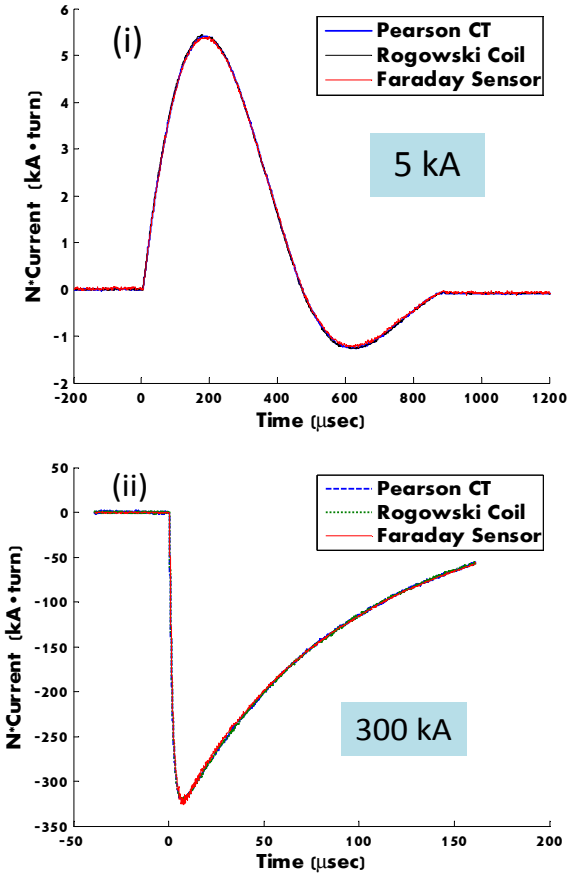

Fig. 8. Good equivalent current (N*I) result comparisons using (i) 49-turn coil and one fiber loop (N=49), and (ii) 3-turn coil and 28 fiber loops (N=3*28=84).

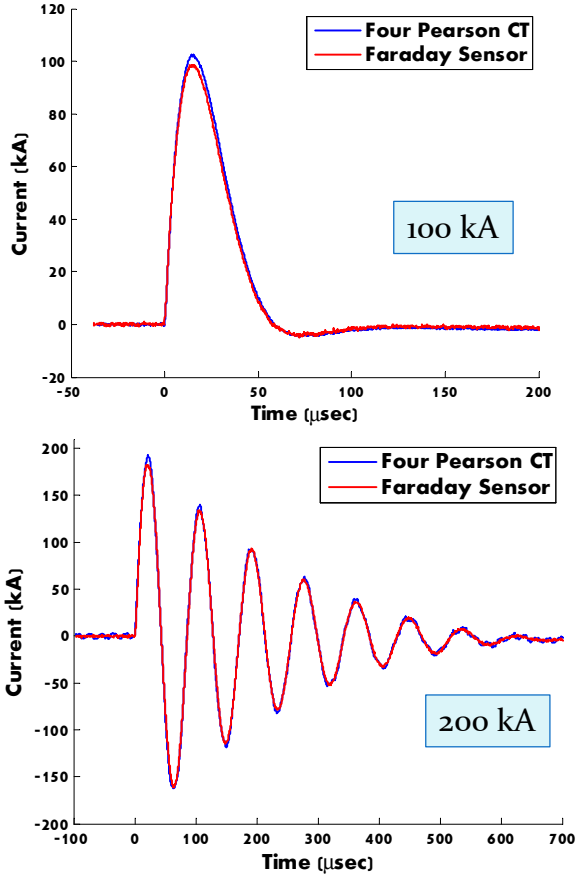

Fig. 10. Reasonable comparison achieved measuring large current (100 kA and 200 kA peaks) despite imperfect setup.

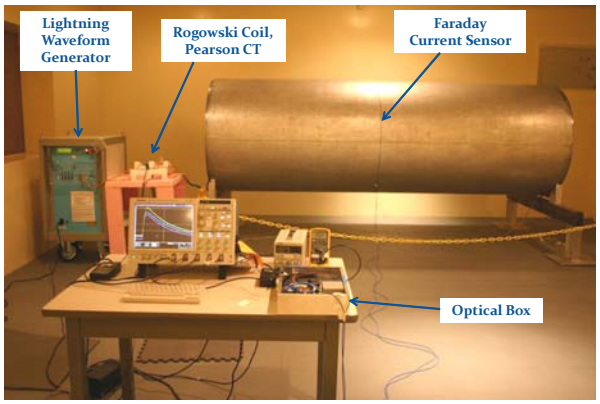

Fig. 11. Measurement on a large aluminum cylinder simulating an aircraft fuselage.

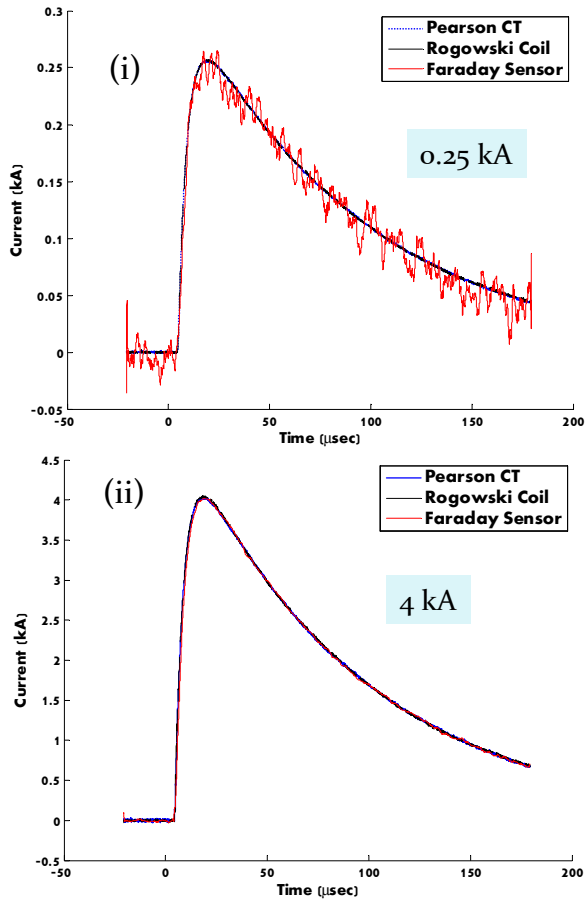

Fig. 12. Current measurement on a 1.2 m diameter cylinder.

Fig. 13. Four loops of fiber optic current sensor installed under the rocket launch tubes.

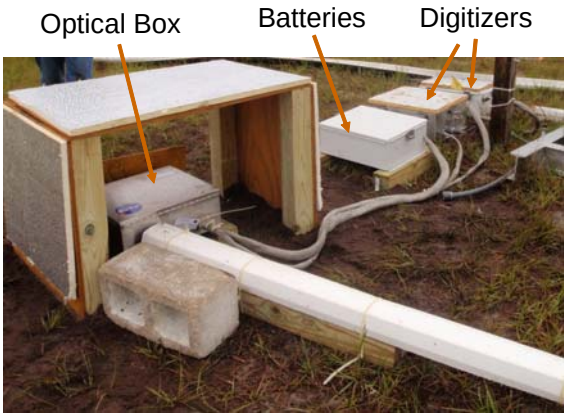

Fig. 14. Optical box and digitizers located 12m from the launch tower.

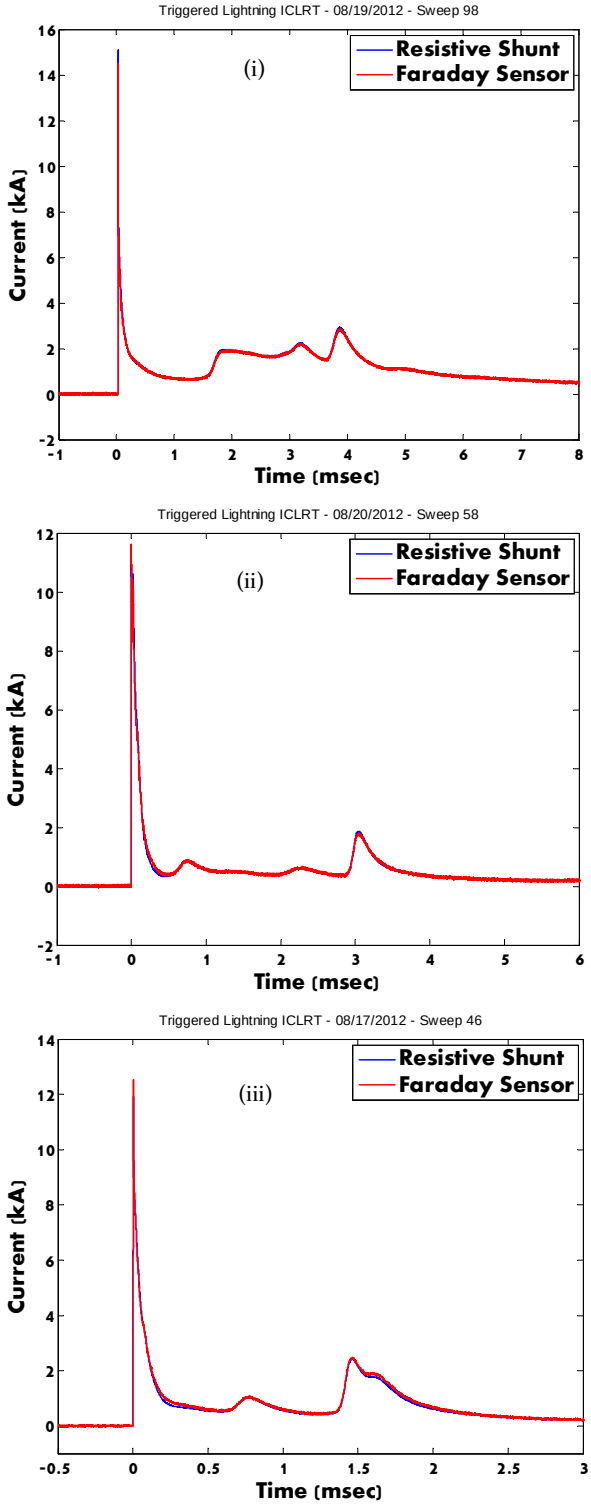

Fig. 15. Results for the 1550nm system show good comparisons with resistive shunt.